

Influence of Voxel Size and Filter Application in Detecting Second Mesio Buccal Canals in Cone-beam Computed Tomographic Images



Sâmia Mouzinho-Machado, MD,*
 Lucas de Paula Lopes Rosado, MD,*
 Fernanda Coelho-Silva, MD,*
 Frederico Sampaio Neves, PhD,*†
 Francisco Haiter-Neto, PhD,*
 and Sergio Lins de Azevedo-Vaz, PhD*‡

ABSTRACT

Introduction: This study assessed the influence of voxel size and filter application in detecting second mesiobuccal (MB2) canals in cone-beam computed tomographic (CBCT) images. **Methods:** Using the OP300 CBCT system (Instrumentarium, Tuusula, Finland) and 3 voxel size protocols (80 μ m, 125 μ m, and 200 μ m), we scanned 40 first molars: 20 with an MB2 canal and 20 without. All molars received silver palladium pins on the palatal root, whereas the non-MB2 molars were also filled with gutta-percha. Five oral radiologists assessed the presence of an MB2 canal under 3 filter application conditions: without filter, with sharpen 1 \times filter, and with sharpen 2 \times filter. Intra- and interobserver reproducibility was evaluated using the weighted kappa index. We compared the area under the receiver operating characteristic curves with SPSS Statistics v.20.0 (IBM Corp, Armonk, NY) using 2-way analysis of variance and the Tukey post hoc test with 5% significance level. **Results:** Our analysis found median intra- and interobserver agreement values of 0.70 and 0.56, respectively. The 80- μ m voxel with sharpen 1 \times filter image group had the highest sensitivity, accuracy, and negative predictive values. As for specificity and positive predictive, the 80- μ m voxel group without filter application presented the highest values. The areas under the receiver operating characteristic curve were higher in the 80- μ m groups than in the 125- μ m and 200- μ m voxel size groups ($P < .05$). We found no differences among the filters used ($P = .22$) or for the filter-voxel size interactions ($P = .88$). **Conclusions:** A smaller voxel size increased the accuracy in detecting MB2 canals, whereas the enhancement filters did not. (*J Endod* 2021;47:1391–1397.)

KEY WORDS

Cone-beam computed tomography; diagnostic imaging; endodontics; molar; radiographic image enhancement

Proper knowledge regarding the root canal system morphology is essential to avoid incomplete instrumentation, 1 of the key factors leading to failed endodontic treatments. Such a failure can result in signs and symptoms related to microbial proliferation, such as pain and a sinus tract^{1–4}. Maxillary molars, the teeth that undergo the most endodontic treatment, often require retreatment due to failure in second mesiobuccal (MB2) canal detection^{5–7}. The MB2 canal is regularly present in first maxillary molars, with a prevalence of 69.6%⁸. Besides the frequency of missed MB2 canals in initial endodontic treatment, rehabilitation of compromised teeth usually uses metallic materials, such as pins of different chemical elements, that can interfere in detecting a particular structure or condition^{9–12}.

In this context, the American Association of Endodontists recommends using cone-beam computed tomographic (CBCT) to analyze teeth with potential extra canals and for those that may require retreatment¹³. In turn, the European Society of Endodontology indicates CBCT imaging for relapsing cases with possible untreated canals¹⁴.

In the context of CBCT image acquisition, a dixel is defined as the smallest unit at the image receptor of a given machine. Before creating a 3-dimensional image, bidimensional images called basis

SIGNIFICANCE

We believe our study can contribute to this clinical area by showing if there is a possibility of radiation dose reduction when using both voxel size and filter application variations in MB2 canal detection.

From the *Division of Oral Radiology, Department of Oral Diagnosis, Piracicaba Dental School, University of Campinas, Piracicaba, São Paulo, Brazil;

†Department of Propedeutics and Integrated Clinic, Division of Oral Radiology, Federal University of Bahia, Salvador, Bahia, Brazil; and ‡Department of Clinical Dentistry, Federal University of Espírito Santo, Vitória, Espírito Santo, Brazil

Address requests for reprints to Dr Sergio Lins de Azevedo-Vaz, Division of Oral Radiology, Department of Oral Diagnosis, Piracicaba Dental School, University of Campinas, Av Limeira 901, CEP 13414-903, Piracicaba, SP, Brazil.

E-mail address: sergiolinsv@gmail.com
 0099-2399/\$ - see front matter

Copyright © 2021 American Association of Endodontists.

<https://doi.org/10.1016/j.joen.2021.06.011>

images are generated by the system; these have the pixel as their smallest constituent unit. When reconstructing these images, the CBCT system produces a digital volume composed by voxels. In addition, CBCT software may have a thickness changing tool, which groups several slices with the originally acquired voxel size to form an image of a thicker slice. This technique usually allows a certain level of adjustment in protocol creation, such as changing the voxel size¹⁵. Research suggests that a smaller voxel size results in higher diagnostic accuracy for MB2 canal detection^{16,17}. However, using a smaller voxel size generally requires higher X-ray radiation doses because of the automatic adjustment of parameters such as milliamperage or field of view¹⁵.

The software used to analyze CBCT images usually allows the application of enhancement filters, which are tools that modify the images by smoothing (blurring of structure limits), sharpening (increased definition of anatomic boundaries), and changing color, among others. Some software and filters have shown higher accuracy in detecting transverse root fracture¹⁸ and measuring apical bone loss¹⁹. These findings suggest that filter application can be used in conjunction with larger voxel sizes to achieve similar diagnostic accuracy to that offered by smaller ones, effectively reducing the radiation dose. Such a hypothesis supports the newest principle of radiation dose optimization for imaging examinations, which is based on reducing the dose to “as low as diagnostically acceptable, being indication-oriented, and patient-specific” (ALADAIP)²⁰. To the best of our knowledge, there are no studies on enhancement filters associated with different voxel sizes for MB2 canal detection. Thus, the aim in this study was to evaluate the influence of both these parameters (voxels and filters) on MB2 canal detection.

MATERIALS AND METHODS

This was an experimental *in vitro* study conducted after approval by the local research ethics committee (CAAE 25098619.1.0000.5418).

Sample Size and Preparation

Our study included a total of 40 maxillary first molars, 20 with an MB2 canal (test group) and 20 without it (control group), whose collection, preparation, and phantom construction were conducted following the work of Rosado et al²¹. The reference standard adopted to

determine the presence or absence of an MB2 canal were micro-computed tomographic images taken with the Skyscan 1174 (Bruker, Kontich, Belgium) using the following parameters: 31.03- μ m voxel size, 50 kVp, 800 μ A, 0.5-mm aluminum filter, 0.5° rotation step, 180° arch rotation, and 1 frame averaging. Silver palladium pins 20-mm long with the same thickness as the files used during instrumentation (025.07) were inserted into the palatal canals up to two thirds of the root length. Gutta-percha was inserted into the other instrumented canals, which excludes the MB2 canal. The control group also received gutta-percha up to the working length.

Image Acquisition

Tomographic images of the teeth were taken with the OP300 Maxio CBCT system (Instrumentarium, Tuusula, Finland) to obtain images with 80- μ m, 125- μ m, and 200- μ m voxel sizes. The kilovoltage and field of view were 90 kVp and 50 \times 50 mm, respectively. Milliamperage and exposure time automatically varied according to the selected voxel size as follows: 5 mA and 8.7 seconds (80 μ m), 6.3 mA and 6.09 seconds (125 μ m), and 8 mA and 2.34 seconds (200 μ m). Because of the difference in exposure parameters, the dose area products were, from smaller to largest voxel size protocols, 377, 332, and 162 mGycm² (Instrumentarium).

Image Evaluation

For evaluation, we exported the images in the Digital Imaging and Communications in Medicine format from CliniView (Instrumentarium) and imported them into OnDemand 3D (Cybermed Inc, Seoul, Republic of Korea). Each tomographic volume underwent 3 filter application conditions: no filter, sharpen 1 \times filter, and sharpen 2 \times filter. The combination of 3 voxel sizes and 3 filter application protocols generated 9 experimental groups (resulting in a total of 360 images): no filter, 80- μ m voxel size (NF-80); no filter, 125- μ m voxel size (NF-125); no filter, 200- μ m voxel size (NF-200); sharpen 1 \times filter, 80- μ m voxel size (S1-80); sharpen 1 \times filter, 125- μ m voxel size (S1-125); sharpen 1 \times filter, 200- μ m voxel size (S1-200); sharpen 2 \times filter, 80- μ m voxel size (S2-80); sharpen 2 \times filter, 125- μ m voxel size (S2-125); and sharpen 2 \times filter, 200- μ m voxel size (S2-200) (Fig. 1).

Five previously calibrated oral radiologists with a minimum of 2 years of experience with CBCT diagnosis blindly evaluated the images regarding the presence or absence of an MB2 canal on LCD monitors

in a dimly lit room. They were allowed to adjust zoom, brightness, and contrast at their discretion and used a 5-point scale to verify an MB2 canal: 1, definitely absent; 2, probably absent; 3, uncertain; 4, probably present; and 5, definitely present. Thirty days after the first evaluation, 40% of the sample was reevaluated to calculate intraobserver reproducibility.

Statistical Analysis

Intra- and interobserver reproducibilities were measured using the weighted kappa index. We calculated sensitivity, specificity, positive predictive value (PPV), negative predictive value (NPV), and accuracy values for each experimental group. These values had the following clinical interpretation herein: sensitivity, reflecting the rate at which the MB2 canal was correctly classified as “present”; specificity, referring to the correct “absent” classification; accuracy, concerning the precision with which the findings reflect the real situation; and PPV and NPV, reflecting the probability of the evaluator correctly classifying the MB2 canal as present or absent, respectively²².

We also compared the areas under the receiver operating characteristic (ROC) curves among the experimental groups using 2-way factorial analysis of variance and the Tukey post hoc test. ROC curve analysis shows the sensitivity values on the y-axis and 1 – specificity values on the x-axis; thus, the location of the ROC curves that represent higher accuracy in the diagnostic task studied is in the upper left region of the graph²³. Analyses were performed using SPSS Statistics Version 20.0 (IBM SPSS Statistics for Windows; IBM Corp, Armonk, NY) at a 5% significance level. The hypothesis tested was that the experimental groups with 125- μ m and 200- μ m voxel sizes with filter application (S1-125, S2-125, S1-200, and S2-200) would show the same accuracy in detecting the MB2 canal as the 80- μ m voxel size groups.

RESULTS

Our analysis found median intra- and interobserver agreement values of 0.70 (ranging from 0.32–0.97) and 0.56 (ranging from 0.21–0.90), respectively. Table 1 presents the agreement value range per experimental group.

Group S1-80 presented the highest values of sensitivity, accuracy, and NPV, whereas NF-80 had the highest values of specificity and PPV. We found the highest

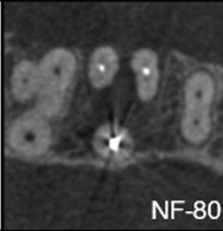
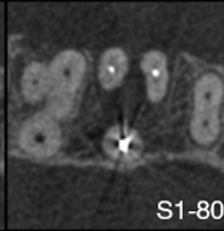
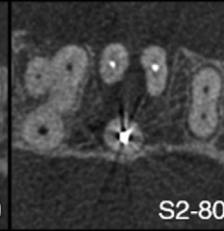
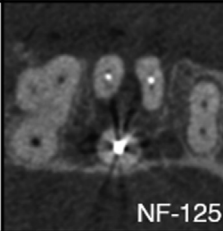
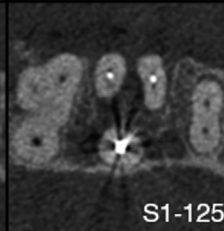
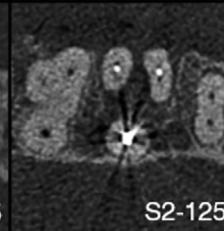
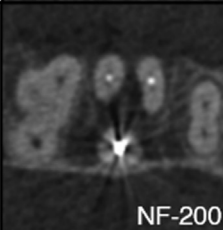
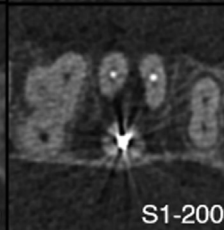
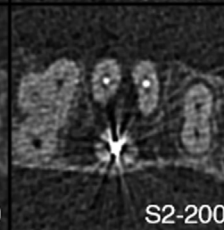
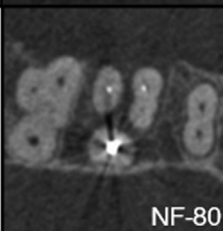
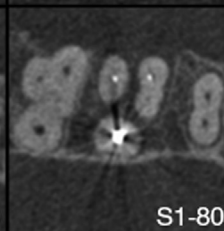
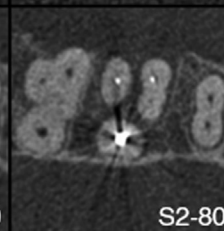
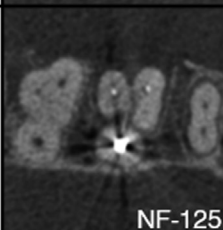
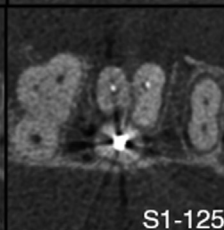
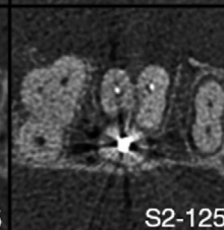

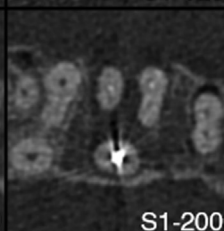
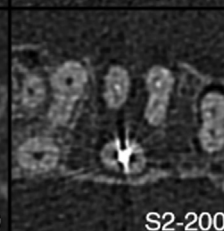
		No filter	Sharpen 1x	Sharpen 2x
Without MB2 canal	80 μ m voxel size	 NF-80	 S1-80	 S2-80
	125 μ m voxel size	 NF-125	 S1-125	 S2-125
	200 μ m voxel size	 NF-200	 S1-200	 S2-200
With MB2 canal	80 μ m voxel size	 NF-80	 S1-80	 S2-80
	125 μ m voxel size	 NF-125	 S1-125	 S2-125
	200 μ m voxel size	 NF-200	 S1-200	 S2-200

FIGURE 1 – Axial reconstructions showing images of the 9 experimental groups and acronyms in examples without and with the presence of an MB2 canal. NF, no filter; S1, sharpen 1 \times ; S2, sharpen 2 \times ; 80, 80- μ m voxel size; 125, 125- μ m voxel size; and 200, 200- μ m voxel size.

areas under the ROC curve values in the NF-80 (0.91), S1-80 (0.94), and S2-80 (0.93) groups. The 80- μ m voxel size groups (NF-80, S1-80, and S2-80) showed higher values than the 125- μ m (NF-125, S1-125, and S2-125) and 200- μ m (NF-200, S1-200, and S2-200) voxel

size groups ($P < .05$). We found no differences between the 125- μ m and 200- μ m groups ($P > .05$), and no statistically significant differences among the filters used and for the filter-voxel size interaction ($P > .05$) (Table 2, Fig. 2).

DISCUSSION

The presence of an MB2 canal can interfere with the endodontic treatment success as observed by the high frequency of maxillary molars that need retreatment due to failure in

TABLE 1 - The Minimum, Maximum, and Median Kappa Values for Intra- and Interobserver Reproducibility

Protocols	Intraobserver			Interobserver		
	Minimum	Maximum	Median	Minimum	Maximum	Median
NF-80	0.33	0.64	0.58	0.30	0.70	0.57
S1-80	0.36	0.77	0.72	0.50	0.78	0.65
S2-80	0.80	0.97	0.90	0.42	0.77	0.70
NF-125	0.57	0.89	0.77	0.25	0.67	0.49
S1-125	0.44	0.90	0.65	0.38	0.90	0.63
S2-125	0.32	0.55	0.42	0.42	0.74	0.61
NF-200	0.55	0.84	0.69	0.28	0.74	0.46
S1-200	0.61	0.90	0.73	0.37	0.76	0.52
S2-200	0.49	0.87	0.83	0.21	0.67	0.40
All groups	0.32	0.97	0.70	0.21	0.90	0.56

NF-80, 80- μ m voxel size, no filter; NF-125, 125- μ m voxel size, no filter; NF-200, 200- μ m voxel size, no filter; S1-80, 80- μ m voxel size, Sharpen 1 \times ; S2-80, 80- μ m voxel size, Sharpen 2 \times ; S1-125, 125- μ m voxel size, Sharpen 1 \times ; S2-125, 125- μ m voxel size, Sharpen 2 \times ; S1-200, 200- μ m voxel size, Sharpen 1 \times ; S2-200, 200- μ m voxel size, Sharpen 2 \times .

detecting the MB2 canal⁷. Thus, our study aimed to use different combinations of enhancement filters and voxel sizes to assess the best protocol to detect an MB2 canal in maxillary molars with endodontic and prosthetic treatment.

Rehabilitation of compromised teeth often requires the use of metallic materials, such as extra- and intracanal posts of different chemical elements, a variable that can affect diagnostic tasks^{9–12}. One of the many issues relative to this metallic material influence is the beam hardening effect, in which materials of high atomic number, such as metals, absorb the lower-energy rays from the polychromatic spectrum emitted by the X-ray machine. Such absorption results in the recording of lower mean beam energy and subsequent dark streak formation (ie, artifacts) because of an error in the 3-dimensional reconstruction²⁴. Although the formation of artifacts was noticeable in the images under analysis, studying the metallic material influence in MB2 canal detection

was not our goal; rather, we aimed to simulate a common clinical scenario in which endodontically treated teeth restoration includes intracanal pins. Because Rosado et al²¹ found no influence of different intracanal materials in MB2 canal detection, we selected only 1 type of material—the silver palladium pins.

Our findings showed higher accuracy for MB2 canal detection in the experimental groups with smaller voxel sizes, probably due to greater imaging detail and differentiation of smaller structures¹⁵. Other studies have tested the influence of voxel size on different diagnostic tasks, with the results varying according to the task and the CBCT systems used^{10,11,25–31}. Despite the fact that the general influence of voxel size remains inconclusive, Bauman et al¹⁶ and Vizzotto et al¹⁷ also found higher accuracy in MB2 canal detection while using smaller voxel sizes in some of the study groups although without applying filters or considering their influence on this diagnostic task.

TABLE 2 - Diagnostic Values and Comparison of the Area Under the Receiver Operating Characteristic Curve (AUC) Values among the Experimental Groups

Protocols	Sensitivity	Specificity	Accuracy	PPV	NPV	AUC
NF-80	87.0	90.0	88.5	89.6	87.3	0.91*
S1-80	95.0	86.0	90.5	87.1	94.5	0.94*
S2-80	90.0	89.0	89.5	89.1	89.9	0.93*
NF-125	79.0	85.0	82.0	84.0	80.1	0.85
S1-125	86.0	85.0	85.5	85.1	85.8	0.90
S2-125	82.0	88.0	85.0	87.2	83.0	0.88
NF-200	84.0	79.0	81.5	80.0	83.1	0.84
S1-200	89.0	74.0	81.5	77.3	87.0	0.87
S2-200	86.0	76.0	81.0	78.1	84.4	0.87

NF-80, 80- μ m voxel size, no filter; NF-125, 125- μ m voxel size, no filter; NF-200, 200- μ m voxel size, no filter; NPV, negative predictive value; PPV, positive predictive value; S1-80, 80- μ m voxel size, Sharpen 1 \times ; S2-80, 80- μ m voxel size, Sharpen 2 \times ; S1-125, 125- μ m voxel size, Sharpen 1 \times ; S2-125, 125- μ m voxel size, Sharpen 2 \times ; S1-200, 200- μ m voxel size, Sharpen 1 \times ; S2-200, 200- μ m voxel size, Sharpen 2 \times .

*A statistically significant difference ($P < .05$) among the given voxel size protocol and the others, considering the same filter condition. We found no statistically significant differences among filters or for the filter–voxel size interaction ($P > .05$).

Sharpening filters, a variety of high-pass filters, are tools used to enhance high-frequency image content while reducing low-frequency ones. Applying these filters leads to a voxel output with an altered gray scale relative to the original values. Because sharpening filters generally increase image contrast and highlight structure boundaries, we applied the Sharpen 1 \times and Sharpen 2 \times filters to increase MB2 canal detection, with the latter having a more intense effect on the image^{32,33}. However, contrary to our initial hypothesis, the application of those filters had no influence on MB2 canal detection in images with 80- μ m, 125- μ m, and 200- μ m voxel sizes. Although some studies also suggest no influence of filter application on tasks related to root and root canal conditions^{9,10,34–36}, other research shows that filter application significantly increased the accuracy for detecting transverse root fracture and apical bone loss^{18,19}. These studies show a wide variety of diagnostic tasks, visualization software, filters, and a general lack of detailed information on image processing, perhaps due to copyright, hence the difficulty in comparing results among studies using different CBCT systems and software. Nonetheless, the literature suggests that filters can potentially influence specific diagnostic tasks.

Our results showed that the 80- μ m voxel size groups had the highest diagnostic values—specificity and PPV in NF-80 and sensitivity, accuracy, and NPV in S1-80. Because the differences among the NF-80 and S1-80 diagnostic values were low, this finding suggests that applying a sharpening filter slightly increased MB2 canal detection, thus increasing the sensitivity values but also the image noise. Higher image noise values can lead to extra false-positive diagnoses and consequently to lower PPV and higher NPV.

NF-125, in turn, had the lowest sensitivity and NPV values; S1-200 the lowest specificity and PPV values; and S2-200 the lowest accuracy. In the S1-200 group, similar to what may have happened to the S1-80 group, a higher amount of noise may have increased MB2 canal detection and false-positive diagnoses, decreasing PPV and increasing NPV. Applying the Sharpen 2 \times filter to the 200- μ m voxel group (S2-200) may have degraded the image resolution, decreasing the accuracy values. These results did not corroborate our hypothesis; we expected that applying sharpening filters would increase diagnostic values for MB2 canal detection using larger voxel sizes.

While analyzing the areas under the ROC curves, we found no statistically significant differences among the filters used and for the filter–voxel size interaction.

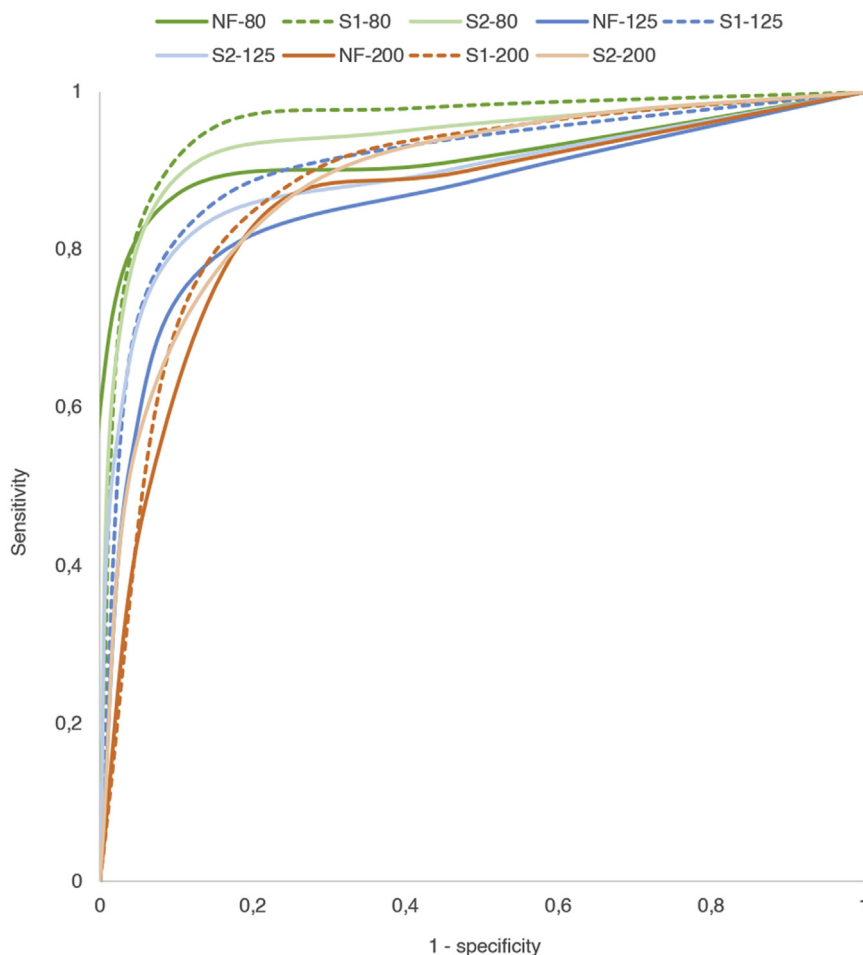


FIGURE 2 – ROC curves generated in the study. The *green, blue, and orange lines* represent the 80- μm , 125- μm , and 200- μm voxel groups, whereas the *continuous dark, dashed dark, and continuous light lines* represent the no filter, Sharpen 1 \times , and Sharpen 2 \times groups, respectively.

Regarding voxel size, the 80- μm groups had the highest areas under the ROC curve values (ie, NF-80 [0.91], S1-80 [0.94], and S2-80 [0.93]). Although the 80- μm voxel size groups (NF-80, S1-80, and S2-80) showed significantly higher values than the 125- μm (NF-125, S1-125, and S2-125) and 200- μm (NF-200, S1-200, and S2-200) groups, the lowest area under the ROC curve was 0.84 (NF-200), meaning that all values can at least be considered excellent³⁷. We also consider the possibility that the selected study design overestimates the observed diagnostic values.

As *in vitro* research, our study design lacks clinical information, signs, symptoms, and patient characteristics such as intrinsic movements, which could aid or hinder the diagnostic task. Despite these limitations, the design presented a valuable option, allowing the multiple and successive CBCT acquisitions necessary to achieve our goals, which are unfeasible in a clinical study because of ethical issues. A controlled *in vitro* study also allows us to reduce variables unrelated to the study objectives and the risk of bias. Although our study showed interference of different voxel sizes with MB2 canal detection on the OP300

CBCT system, no impact of filter application on OnDemand 3D, and no interaction among filters and voxel sizes, studies using other systems and software may yield different results.

CONCLUSION

A smaller voxel size increased the accuracy in detecting the MB2 canal, whereas enhancement filters had no influence on the accuracy for this diagnostic task. Consequently, CBCT images with 125- μm and 200- μm voxel sizes with filter application did not show the same accuracy in MB2 canal detection as images with 80- μm voxel size.

CREDIT AUTHORSHIP CONTRIBUTION STATEMENT

Sâmia Mouzinho-Machado:

Conceptualization, Data curation, Formal analysis, Investigation, Methodology, Project administration, Visualization, Writing - original draft. **Lucas de Paula Lopes Rosado:**

Conceptualization, Investigation, Methodology, Resources, Writing - original draft. **Fernanda Coelho-Silva:**

Data curation, Formal analysis, Methodology, Investigation, Writing - original draft. **Frederico Sampaio Neves:**

Conceptualization, Methodology, Resources, Supervision, Writing - review & editing. **Francisco Haiter-Neto:**

Conceptualization, Methodology, Supervision, Writing - review & editing. **Sergio Lins de-Azevedo-Vaz:**

Conceptualization, Data curation, Formal analysis, Methodology, Supervision, Visualization, Project administration, Writing - review & editing.

ACKNOWLEDGMENTS

The authors thank Espaço da Escrita–Pró-Reitoria de Pesquisa for the language services provided.

Funding: Coordenação de Aperfeiçoamento de Pessoal de Nível Superior (finance code 001).

The authors deny any conflicts of interest related to this study.

REFERENCES

1. López-Marcos JF. Aetiology, classification and pathogenesis of pulp and periapical disease. *Med Oral Patol Oral Cir Bucal* 2004;9(Suppl 1):58–62. 52–57.

2. Yu C, Abbott PV. An overview of the dental pulp: Its functions and responses to injury. *Aust Dent J* 2007;52(Suppl):S4–6.
3. Zhang Y, Xu H, Wang D, et al. Assessment of the second mesiobuccal root canal in maxillary first molars: a cone-beam computed tomographic study. *J Endod* 2017;43:1990–6.
4. Kim Y, Lee D, Kim D-V, Kim S-Y. Analysis of cause of endodontic failure of C-shaped root canals. *Scanning* 2018;2018:2516832.
5. Witherspoon DE, Small JC, Regan JD. Missed canal systems are the most likely basis for endodontic retreatment of molars. *Tex Dent J* 2013;130:127–39.
6. Studebaker B, Hollender L, Mancil L, et al. The incidence of second mesiobuccal canals located in maxillary molars with the aid of cone-beam computed tomography. *J Endod* 2018;44:565–70.
7. do Carmo WD, Verner FS, Aguiar LM, et al. Missed canals in endodontically treated maxillary molars of a Brazilian subpopulation: prevalence and association with periapical lesion using cone-beam computed tomography. *Clin Oral Investig* 2021;25:2317–23.
8. Martins JN, Marques D, Silva EJ, et al. Second mesiobuccal root canal in maxillary molars—a systematic review and meta-analysis of prevalence studies using cone beam computed tomography. *Arch Oral Biol* 2020;113:104589.
9. Ferreira LM, Visconti MA, Nascimento HA, et al. Influence of CBCT enhancement filters on diagnosis of vertical root fractures: a simulation study in endodontically treated teeth with and without intracanal posts. *Dentomaxillofac Radiol* 2015;44:2–7.
10. Silva DM, Campos CN, Carvalho AC, Devito KL. Diagnosis of mesiodistal vertical root fractures in teeth with metal posts: influence of applying filters in cone-beam computed tomography images at different resolutions. *J Endod* 2018;44:470–4.
11. Yamamoto-Silva FP, Siqueira Claudéir FO, Silva Maria AG, et al. Influence of voxel size on cone-beam computed tomography-based detection of vertical root fractures in the presence of intracanal metallic posts. *Imaging Sci Dent* 2018;48:177–84.
12. Gaêta-Araujo H, Nascimento EH, Oliveira-Santos N, et al. Influence of adjacent teeth restored with metal posts in the detection of simulated internal root resorption using CBCT. *Int Endod J* 2020;53:1299–306.
13. Special Committee to Revise the Joint AAE/AAOMR Position Statement on use of CBCT in Endodontics. AAE and AAOMR joint position statement: use of cone beam computed tomography in endodontics 2015 update. *J Endod* 2015;120:508–12.
14. Patel S, Brown J, Semper M, et al. European Society of Endodontology position statement: use of cone beam computed tomography in endodontics: European Society of Endodontology (ESE) developed by Int Endod J 2019;52:1675–8.
15. Pauwels R, Araki K, Siewersden JH, Thongvigitmanee SS. Technical aspects of dental CBCT: state of the art. *Dentomaxillofac Radiol* 2015;44:20140224.
16. Bauman R, Scarfe W, Clark SJ, et al. *Ex vivo* detection of mesiobuccal canals in maxillary molars using CBCT at four different isotropic voxel dimensions. *Int Endod J* 2011;44:752–8.
17. Vizzotto MB, Silveira PF, Arús NA, et al. CBCT for the assessment of second mesiobuccal (MB2) canals in maxillary molar teeth: effect of voxel size and presence of root filling. *Int Endod J* 2013;46:870–6.
18. Wenzel A, Haiteir-Neto F, Frydenberg M, Kirkevang LL. Variable-resolution cone-beam computerized tomography with enhancement filtration compared with intraoral photostimulable phosphor radiography in detection of transverse root fractures in an *in vitro* model. *Oral Surg Oral Med Oral Pathol Oral Radiol Endod* 2009;108:939–45.
19. de Sousa ET, Pinheiro MA, Maciel PP, Sales Marcelo AO. Influence of enhancement filters in apical bone loss measurement: a cone-beam computed tomography study. *J Clin Exp Dent* 2017;9:e516–9.
20. Oenning AC, Jacobs R, Pauwels R, et al. Cone-beam CT in paediatric dentistry: DIMITRA project position statement. *Pediatr Radiol* 2018;48:308–16.
21. Rosado LP, Fagundes FB, Freitas DQ, et al. Influence of the intracanal material and metal artifact reduction tool in the detection of the second mesiobuccal canal in cone-beam computed tomographic examinations. *J Endod* 2020;46:1067–73.
22. Hannu H. Caries prediction - state of the art. *Community Dent Oral Epidemiol* 1997;25:87–96.
23. Hui HZ, Jane C, Dawn T. What is an ROC curve? *Emerg Med J* 2017;34:357–9.
24. Schulze R, Heil U, Groû D, et al. Artefacts in CBCT: a review. *Dentomaxillofac Radiol* 2011;40:265–73.

25. Guo XL, Li G, Zheng JQ, et al. Accuracy of detecting vertical root fractures in non-root filled teeth using cone beam computed tomography: effect of voxel size and fracture width. *Int Endod J* 2019;52:887–98.
26. Serdar U, Gokcen A, Eda Didem Y, et al. The influence of voxel size and artifact reduction on the detection of vertical root fracture in endodontically treated teeth. *Acta Odontol Scand* 2020;0:1–5.
27. Librizzi ZT, Tadinada AS, Valiyaparambil JV, et al. Cone-beam computed tomography to detect erosions of the temporomandibular joint: effect of field of view and voxel size on diagnostic efficacy and effective dose. *Am J Orthod Dentofacial Orthop* 2011;140:e25–30.
28. Icen M, Orhan K, Seker Ç, et al. Comparison of CBCT with different voxel sizes and intraoral scanner for detection of periodontal defects: an *in vitro* study. *Dentomaxillofac Radiol* 2020;49:1–7.
29. Nikneshan S, Valizadeh S, Javanmard A, Alibakhshi L. Effect of voxel size on detection of external root resorption defects using cone beam computed tomography. *Iran J Radiol* 2016;13:e34985.
30. Costa AL, Barbosa BV, Perez-Gomes JP, et al. Influence of voxel size on the accuracy of linear measurements of the condyle in images of cone beam computed tomography: a pilot study. *J Clin Exp Dent* 2018;10:e876–82.
31. Yilmaz F, Sönmez G, Kamburoğlu K, et al. Accuracy of CBCT images in the volumetric assessment of residual root canal filling material: effect of voxel size. *Niger J Clin Pract* 2019;22:1091–8.
32. Analoui M. Radiographic digital image enhancement. Part II: transform domain techniques. *Dentomaxillofac Radiol* 2001;30:65–77.
33. Morihisa S, Yasutaka M, Hayakawa Y, Honda A. Comparison of two - and three-dimensional filtering methods to improve image quality in multiplanar reconstruction of cone-beam computed tomography. *Oral Radiol* 2009;25:154–8.
34. Nascimento MC, Nejaim Y, De Almeida SM, et al. Influence of cone beam CT enhancement filters on diagnosis ability of longitudinal root fractures. *Dentomaxillofac Radiol* 2014;43:3–7.
35. De Azevedo Vaz SL, Vasconcelos TV, Neves FS, et al. Influence of cone-beam computed tomography enhancement filters on diagnosis of simulated external root resorption. *J Endod* 2012;38:305–8.
36. Verner FS, D'Addazio PS, Campos CN, et al. Influence of cone-beam computed tomography filters on diagnosis of simulated endodontic complications. *Int Endod J* 2017;50:1089–96.
37. Mandrekar Jayawant N. Receiver operating characteristic curve in diagnostic test assessment. *J Thorac Oncol* 2010;5:1315–6.